Chemical Engineering Science 251 (2022) 117392

Contents lists available at ScienceDirect

Chemical Engineering Science

journal homepage: www.elsevier.com/locate/ces

Evaluation of hydraulic mixing performance in a full-scale anaerobic digester with an external liquid recirculation system using CFD and experimental validation

Rosario Arnau [a], Javier Climent [a], Raúl Martínez-Cuenca [a], Jorge Rodríguez [b], Sergio Chiva [a,*]

[a] Department of Mechanical Engineering and Construction, Universitat Jaume I, Avd. Vicent Sos Baynat s/n, 12071 Castelló de la Plana, Spain
[b] Department of Chemical Engineering, Research and Innovation Center on CO_2 and H_2 (RICH), Khalifa University, PO Box 127788, Abu Dhabi, United Arab Emirates

HIGHLIGHTS

- CFD anaerobic digesters models were validated by means of complete RTD curve.
- Design mixing parameters in anaerobic digestion should be review.
- Local mixing parameters are strongly recommended for CFD studies.
- Second-order moments offer geometrical and local mixing information in CFD models.
- The propeller was found crucial to avoid dead volumes formation.

GRAPHICAL ABSTRACT

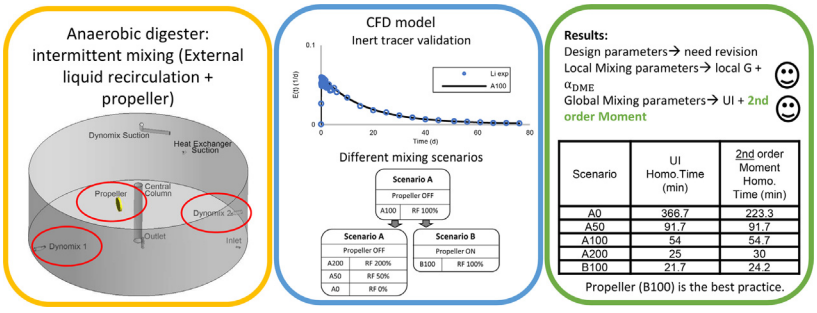

ARTICLE INFO

Article history:
Received 28 July 2021
Received in revised form 7 December 2021
Accepted 20 December 2021
Available online 26 December 2021

Keywords:
Anaerobic digester
CFD
Homogeneity
Mixing degree
Tracer

ABSTRACT

Anaerobic digestion (AD) has become an essential process for sludge treatment and its optimum performance is related to its mixing degree. In this study, a full-scale Anaerobic Digester (ADer) with an external recirculation mixing system was studied via single-phase 3D-CFD simulations to assess the influence of recirculation flow and a 3-blade propeller. The model was validated with inert tracer tests. The design and mixing parameters were studied to characterise the mixing efficiency in different scenarios. The design parameters were assessed first, but wide deviations from the recommended values were found. Local mixing parameters were found to be useful for defining the degree and type of mixing, and are highly recommended in the CFD studies of ADers. A second-order statistical moment was proposed as a global mixing parameter to describe geometrical and local mixing, and to state a reliable homogenisation time.

1. Introduction

Treating the sludge from the conventional activated sludge process is currently one of wastewater treatment plants' (WWTPs) major problems.[1] Presently, one of the preferred processes for carrying out this treatment is anaerobic digestion (AD).[2] A well-functioning AD process consists of multiple microbial reactions in series that sequentially convert the biodegradable organic substrate, such as sludge, into biogas (primarily consisting of methane and carbon dioxide), a nutrient-rich liquid stream and stabilised biosolids (that can be used as fertiliser). More importantly, the net biogas flow is an additional source of renewable energy that can be used to meet not only the energy needs of AD, but also WWTPs' needs (Appels et al., 2008; Tchobanoglous et al., 2003). The microbial community responsible for the process consists of numerous bacteria and archaea which must work in a balanced harmony for the process

* Corresponding author.
E-mail address: schiva@uji.es (S. Chiva).
[1] WWTPs – Wastewater Treatment Plants.
[2] AD – Anaerobic Digestion.

https://doi.org/10.1016/j.ces.2021.117392
0009-2509/

to remain stable (Kleerebezem, 2014). Inadequate mixing can lead to zones with high substrate concentrations, which may bring about the fast local accumulation of acid intermediates or other inhibitors with negative repercussions on the process' effectiveness. As a result, these may, in turn, lead to severe consequences, such as process inhibition and destabilisation.

AD takes place inside enclosed vessels, the so-called anaerobic digesters (ADers),[3] which are designed to meet a hydraulic retention time (HRT)[4] longer than 10 days to ensure the biological treatment of influent organic material. An ADer is also expected to properly mix and homogenise its content (Tchobanoglous et al., 2004). Several design parameters, known as 'rules-of-thumb' (Meroney and Colorado, 2009), have been proposed to provide the dimensions and operating conditions for optimal mixing and homogenization. But their application to real ADers sometimes involves poorly mixed tanks, with short-circuits, apparent inhomogenities, or even dead volume formation. In the worst scenarios, solids' settling may be noticeable and a significant reduction of the HRT can be observed (Monteith and Stephenson, 1981). As a result, the performance of poorly designed ADers is far from the ideally mixed tank that is generally assumed (Terashima et al., 2009).

In practice, these faulty designs are difficult to identify and solve. As the anaerobic atmosphere forces these systems to be sealed, it is not easy to stop these facilities to install proper instrumentation for flow characterisation purposes. One common practice is to follow tracer methods (Cholette and Cloutier, 1959; Levenspiel, 1999; Monteith and Stephenson, 1981) to evaluate overall hydrodynamic performance from the Residence Time Distributions (RTDs).[5] This technique permits the detection of short-circuiting and dead volumes (Meroney and Colorado, 2009; Monteith and Stephenson, 1981; Terashima et al., 2009), but does not provide useful information that can be employed to identify why they take place. In addition, it is difficult to propose solutions based on their results.

Several authors have proposed the use of Computational Fluid Dynamics (CFD)[6] to gain better insight into the hydraulic behaviour of working ADers (Paul et al., 2004). CFD provides detailed 3D descriptions of velocity field and turbulence inside tanks. The visualisation of fluid velocity vectors, streamlines, and/or particle trajectories helps to understand the mixing process and to identify the origin of the faulty hydraulic behaviour in each case (Meroney and Colorado, 2009).

Current research focuses on developing full-scale CFD models to analyse different mixing systems and to evaluate hydraulic defects. Mechanical mixing with impellers in vessels (Bridgeman, 2012; Wu, 2011) and draft tubes (Craig et al., 2013; Meroney and Colorado, 2009) has been studied, while tanks with high velocities and small dead volumes have been reported. Gas mixing has also been addressed on the medium-scale with two-phase CFD models to demonstrate that CFD can explain mixing efficiency with different post-processing tools and parameters (Wu, 2014). Other authors have studied hydraulic mixing with external agitation (Hurtado et al., 2015; Mendoza et al., 2011) and reported maximum velocities of around 0.4 m/s inside a full-scale vessel and the appearance of dead volumes. To reduce energy costs, Hurtado et al., (2015) proposed using intermittent hydraulic mixing, but observed a slight decrease in the active volume. CFD studies on hydraulic mixing (Mendoza et al., 2011) have shown the formation of slow-velocity zones in the bottom centre of tanks, which are defined as dead volumes. It is generally agreed that mechanical mixing is the most efficient mixing system followed by gas mixing, whereas hydraulic mixing with external recirculation is the worst option (Wu, 2010a, 2010b).

ADers' global hydraulic behaviour is complex to analyse. To date, several parameters have been proposed to characterise their hydraulic and mixing performance, as well as the formation of hydraulic defects. Terashima et al., (2009) proposed the Uniformity Index (UI) to characterise the mixing and degree of homogenisation, and the UI has also been used to determine the homogenisation time, i.e. the time needed to accomplish complete mixing (Dapelo and Bridgeman, 2018).

The present work aims to analyse the hydraulic performance of a full-scale ADer with liquid recirculation and mechanical mixing by means of single-phase 3D CFD models. The numerical model was validated using inert tracers. To the authors' knowledge, this is the first time that a complete RTD is employed to check a full-scale ADer's global hydraulic performance and to validate a CFD model. Several mixing CFD scenarios were considered so that the influence of recirculation flow and an internal propeller on the ADer's hydrodynamics could be studied. Additionally, a review of parameters from the literature, such as design parameters (DVTT, UP, and G), local velocity gradient or the UI, was done and applied to different CFD scenarios. Finally, a new global mixing parameter was proposed to establish the mixing parameters of general applications.

2. Materials and methods

An ADer was studied by means of inert tracer experiments and CFD models. The ADer has a DYNOMIX system (external recirculation pump) and an internal propeller as its mixing devices. This ADer was modelled according to a Non-Newtonian single-phase CFD to evaluate different mixing configurations. Several mixing parameters were evaluated through CFD simulations.

2.1. Anaerobic digester description

An ADer (3432 m^3 volume), which is currently installed at a WWTP in Spain, serves as a basis for the simulation and validation elements of this study. Fig. 1 provides a general overview of its geometry and the locations of its internal components. It is of cylindrical shape and its bottom surface is slightly inclined to form a conical geometry.

Table 1 summarises the main tank dimensions as well as the three main flowrates in the system: the feed flow of waste (activated sludge), the heat exchanger flow, and the recirculation flow. The feeding and heat exchanger flows are introduced together into the tank through the inlet nozzle (Fig. 1a). Recirculation is injected using two nozzles (Fig. 1b). The flow leaves the ADer through the outlet, located at the bottom of the tank, close to its axis. The heat exchanger is fed using a suction pipe (Fig. 1c) located close to the wall, 4.2 m over the bottom. Another suction pipe, located near the top of the tank, removes the recirculating flow (Fig. 1d). To provide further mixing, a three-blade submersible propeller (WILO EMU MAXI PROP TR 315.33, 1.5 m-diameter blades, 3.5 kW power) is installed close to the bottom (see Fig. 1a). Table S1 and Figure S1 in the Supplementary Material provide a full description of the facility's dimensions and its internal elements. The depicted central column was initially designed to remove the recirculation flow, but it is no longer used.

The digester operates by alternating two hydrodynamic configurations. In the first one, the DYNOMIX system is active and the propeller is switched off. The facility operates according to this configuration most of the time (162 h per week) and is defined as the base scenario, A100. In the second configuration, the internal propeller is switched on while the DYNOMIX system remains

[3] ADer - Anaerobic Digester.
[4] HRT – Hydraulic Retention Time.
[5] RTDs - Residence Time Distributions.
[6] CFD- Computational Fluid Dynamics.

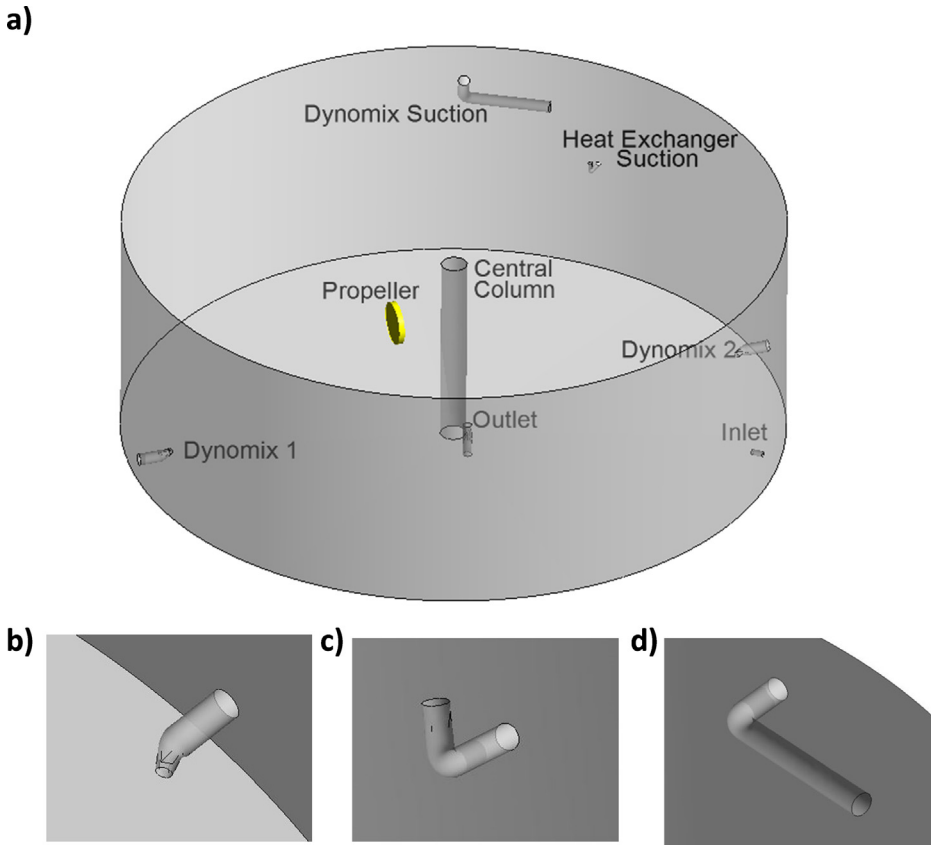

Fig. 1. Details of the digester geometry: (a) overview of the digester with the propeller in yellow; (b) DYNOMIX nozzle; (c) heat exchanger suction pipe; (d) DYNOMIX recirculation suction tube. (For interpretation of the references to colour in this figure legend, the reader is referred to the web version of this article.)

Table 1
Main dimensions and flows of the anaerobic digester.

Paraneter (units)	Value
Diameter (m),$\varnothing_{ADer}$	23
Height of the liquid free surface (m)	8.25
Volume (m^3),V	3432
Feed flow (m^3/h),q_{inlet}	8.3
Heat exchanger flow (m^3/h)	35 (4.2 × the feed flow)
DYNOMIX recirculation flow (m^3/h),q_{recirc}	680 (81.9 × the feed flow)

active. This configuration approximately runs for only 6 h per week and is defined as scenario B100.

2.2. Experimental measurements

A tracer experiment was conducted to experimentally determine the ADer's global hydraulic behaviour. In addition, sludge rheology was characterised by a rotational rheometer.

2.2.1. Hydraulic behaviour study: Tracer test

The overall hydraulic characterization of a full-scale ADer is typically limited to tracer studies. In this case, an experimental tracer test was conducted in Climent et al., (2019). In this test, lithium chloride (LiCl) was employed by the authors to run the test as it is widely used under anaerobic conditions (Dustin and Hansen, 2012; Smith et al., 1993). Batch experiments with LiCl were performed to quantify the tracer's adsortion to ADer solids, which verified that it neither degraded nor adsorbed. Additionally, the background concentrations were measured from the collected influent and effluent samples.

The lithium concentration in the samples was measured. The results are presented in Section 3.3. The mean residence time was obtained to assess the ADer's global mixing performance according to (Levenspiel, 1999):

$$t_m = \frac{\int_0^\infty t \cdot C(t)dt}{\int_0^\infty C(t)dt} = \frac{\sum_{i=1}^\infty t_i \cdot C(t_i)\Delta t_i}{\sum_{i=1}^\infty C(t_i)\Delta t_i} \quad (1)$$

where t_m is the mean residence time (time units) and C and t are the tracer concentration (concentration units) and time (time units), respectively. In an ideally mixed tank (CSTR), t_m and HRT are equal but may differ if hydraulic defects emerge such as short-circuits or dead volumes (Levenspiel, 1999; Li et al., 2017).

2.2.2. Sludge rheology

The rheological characterisation of anaerobic sludge was conducted using a rotational rheometer (Haake RheoStress 1, Thermo Scientific). An anaerobic sludge sample was placed inside the gap between the two concentric cylinders (34 mm and 36.88 mm). The resulting experimental data (see Figure S2) was used to fit an Ostwald-de-Waele submodel (Schramm, 1994):

$$\mu = K\gamma^{n-1} \quad (2)$$

where μ is the apparent viscosity (Pa·s), K is the fluid consistency index (Pa·s^n), γ is the shear rate (s^{-1}), and n is the flow behaviour index (-). The sample had a total solids concentration of 2.67 ± 0.43%. The K and $n-1$ values were fitted as 0.0789 Pa·$s^{0.415}$ and −0.585, respectively.

2.3. Characterization of the anaerobic digester performance

Several parameters in literature describe the performance of mixing in tanks and, here, we briefly introduce the most used ones. For the sake of clarity, these parameters are arranged into four categories, according to their application to design, mixing or defect studies.

2.3.1. Design parameters

The design parameters, usually known as "rules-of-thumb", aim to provide the proper dimensioning of mixing tanks and their operating conditions (Meroney and Colorado, 2009; Tchobanoglous et al., 2004).

- The HRT, calculated in days, is expressed as

$$HRT = \frac{V}{q_{inlet}} \tag{3}$$

where V is the digester's volume (m^3) and q_{inlet} (m^3/day) is the inlet flowrate (not including recirculation). Ideally, the HRT should be similar to the mean residence time obtained from tracer curves. Marked deviations indicate the appearance of hydraulic defects, such as short-circuits or dead volumes.

- The Digester Volume Turnover Time (DVTT), designed in minutes, is obtained as

$$DVTT = \frac{V}{q_{recirc}} \tag{4}$$

where q_{recirc}(m^3/min) stands for the recirculation flow.

- The Unit Power (UP) or Mixing Energy Level (MEL), measured as W/ m^3, is defined as

$$UP = \frac{P}{V} \tag{5}$$

where P is the power input (W), i.e. pumping power.

- The global RMS velocity gradient, $\bar{G}$, measured as s^{-1}, was used as a mixing criterion to quantify the power input needed in an ADer. It can be calculated as

$$\bar{G} = \sqrt{\frac{P}{\mu \times V}} \tag{6}$$

where μ is dynamic viscosity (Pa•s).

The US UEPA (1979) proposed the recommended design parameter values in Table 2 to achieve efficient mixing:

A typical route for designing an ADer would be to set the volume from Eq. (3), and then the recirculation flow and power input from these values and Eqs. (4) to (6).

2.3.2. Local mixing parameters

To estimate the ADer's local mixing degree from the CFD simulations, a local RMS velocity gradient (s^{-1}) can be computed as in (Changgen Luo, 1997; Sindall et al., 2013),

$$G = \sqrt{\frac{\bar{\varepsilon}}{v}} \tag{9}$$

where ε is the energy dissipation per unit mass (m^2/s^3) and v is the kinematic viscosity of fluid (m^2/s). Then the spatial average of the local RMS velocity gradient provides the global RMS velocity gradient defined in Eq. (6).

Table 2
Recommended design parameters. (US EPA, 1979).

HRT(day)	DVTT(min)	UP or MEL(W/m^3)	$\bar{G}(s^{-1})$
15–30	30–45	5–8	50–85

Another parameter to describe the mixing degree locally in the ADer is the dispersive mixing efficiency (α_{DME}) (-). It is described with the following equation (Khapre and Munshi, 2016; Manas-Zloczower, 1994):

$$\alpha_{DME} = \frac{\|\dot{\gamma}\|}{\|\dot{\gamma}\| + \|\omega\|} \tag{10}$$

where $\dot{\gamma}$ is the strain tensor rate and ω is the vorticity tensor. Both variables are available in the numerical simulations. This relates to the type of deformation that the fluid undergoes inside the tank: on the one hand, the deformation caused by elongation or symmetric deformation is defined by the shear rate; on the other hand, the antisymmetrical deformation caused by the irrotational flow is described by the vorticity tensor. The value of this parameter can define the type of flow that produces mixing inside the vessel as:

- $\alpha_{DME} = 0$ for pure rotation, no effective mixing or rotational flow
- $\alpha_{DME} = 0.5$ for shear flow
- $\alpha_{DME} = 1$ for dispersive flow by pure elongation

As the local mixing parameters can be computed at every cell of the numerical simulation, they provide more information on both mixing efficiency and mixing type than others.

2.3.3. Global mixing parameters

One of the major concerns in studying ADs is their ability to homogeneously mix their content. Hence developing a set of performance parameters that allow for the quantification of how well a given ADer is mixed is worthwhile. The global RMS velocity gradient is typically used as a design parameter, but lacks generality because the required value depends on vessel size and the configuration of its internals. Employing CFD simulations provides better insight into AD behaviour by offering a definition of new more relevant mixing parameters. As this set of parameters is calculated from the local characteristics of flow, their formulation is expected to be of general applicability. The global mixing parameters presented in this section need inert tracer experience to be studied, which is quite normal in CFD studies. The description of this experience is detailed in Section 2.4.3.2.

Terashima et al. (2009) proposed the first mixing parameter for AD based on CFD simulations: the Uniformity Index (UI) (-). Later it was modified (Dapelo and Bridgeman, 2018) to be calculated as

$$UI = \frac{\sum_{i=1}^{m} \left\{ \left| C_i - \bar{C} \right| V_i \right\}}{2V\bar{C}} \tag{11}$$

where V_i is the cell volume (m^3), C_i is the cell tracer concentration (ppm), and $\bar{C}$ is the average tracer volume concentration (ppm), computed as:

$$\bar{C} = \frac{\sum_{i=1}^{m} C_i V_i}{V} \tag{12}$$

Note that the UI takes 1 as the maximum value when the whole tracer is located in only one cell (completely and non-uniformly distributed), and it equals 0 when the tracer is homogeneously distributed in the region (the same concentration in every cell). According to Terashima et al., (2009), a homogenisation time, t_{UI}

(time) can be defined as the time until the UI reaches a value of 0.01 (-) (0.99 percentile). The UI only describes how much the digester is mixed globally, but not how it has been reached.

Thus we propose using a new set of mixing parameters based on the Moments Theory (Papoulis, 1984). Central moments are a valuable mathematical tool to characterise the location, spread and shape of mathematical distributions, such as the tracer concentration, in the ADers volume. As first-order moments account for the location of the distribution centroid, they are expected to change over time as the tracer pulse advances. First-order central moments account for the location of the distribution centroid. By means of cylindrical coordinates (r, θ, z), they can be calculated as:

$$\bar{r}(t) = \frac{1}{V\bar{C}} \int_{CV} r\, C(r,\theta,z,t)\, dV \tag{13}$$

$$\bar{\theta}(t) = \frac{1}{V\bar{C}} \int_{CV} \theta\, C(r,\theta,z,t)\, dV \tag{14}$$

$$\bar{z}(t) = \frac{1}{V\bar{C}} \int_{CV} z\, C(r,\theta,z,t)\, dV \tag{15}$$

Second-order central moments are related to the distribution spread and can be computed as:

$$\sigma_r^2(t) = \frac{1}{V\bar{C}} \int_{CV} \left(r-\bar{r}\right)^2 C(r,\theta,z,t)\, dV \tag{16}$$

$$\sigma_\theta^2(t) = \frac{1}{V\bar{C}} \int_{CV} \left(\theta-\bar{\theta}\right)^2 C(r,\theta,z,t)\, dV \tag{17}$$

$$\sigma_z^2(t) = \frac{1}{V\bar{C}} \int_{CV} \left(z-\bar{z}\right)^2 C(r,\theta,z,t)\, dV \tag{18}$$

Note that the second-order moment for the azimuthal component cannot be directly compared to those for the radial and axial directions because they have different units. To make them comparable, the following dimensionalised version of the moment is applied:

$$\widehat{\sigma}_\theta^2(t) = \bar{r}^2(t)\sigma_\theta^2(t) \tag{19}$$

As a result of this dimensionalisation, this moment can be interpreted as the width of the distribution across the azimuthal direction and can be compared to the radial and axial widths.

With this set of second-order moments, it is easy to check if mixing is performed isotropically or not. This is the major benefit over the UI because second-order moments show the direction that encourages ADers' homogenisation. Furthermore, it is possible to quantify the degree of homogenisation. When the tracer pulse enters the domain, these moments are nearly zero as the tracer is localised in the inlet region. As time elapses, the tracer starts to spread and these moments increase. Eventually, the tracer can be homogeneously distributed with a constant value throughout the domain, i.e. $C(r,\theta,z,t) = \bar{C}$. When the tracer is homogeneously distributed and remains stationary, these moments become $\sigma_{r,h}^2, \widehat{\sigma}_{\theta,h}^2, \sigma_{z,h}^2$, and can be expressed as:

$$\sigma_{r,h}^2 = \frac{1}{V} \int_{CV} \left(r-\bar{r}\right)^2 dV \tag{20}$$

$$\hat{\sigma}_{\theta,h}^2 = \frac{\sigma_{r,h}^2}{V} \int_{CV} \left(\theta-\bar{\theta}\right)^2 dV \tag{21}$$

$$\sigma_{z,h}^2 = \frac{1}{V} \int_{CV} \left(z-\bar{z}\right)^2 dV \tag{22}$$

This leads to the definition of a set of normalised second-order central moments with an initial value of 0 and a homogeneous value of 1, as so:

$$\sigma_r^2(t) = \frac{\sigma_r^2(t)}{\sigma_{r,h}^2} \tag{23}$$

$$\sigma_\theta^2(t) = \frac{\widehat{\sigma}_\theta^2(t)}{\widehat{\sigma}_{\theta,h}^2} \tag{24}$$

$$\sigma_z^2(t) = \frac{\sigma_z^2(t)}{\sigma_{z,h}^2} \tag{25}$$

From this definition, a homogenisation time can be estimated as the time when all the normalised second-order moments remain over 0.99.

2.4. Modelling

Numerical simulations were done according to commercial computational fluid dynamics code ANSYS CFX 17.2. (ANSYS CFX, 2017). All the simulations were solved via parallel computing with eight processes in a computer with an Intel Core i7-3770 processor (3.40 GHz) and 32 Gb RAM.

2.4.1. Model geometry and meshing

3D geometry was reproduced and vessel geometry and nozzles were introduced in detail (Fig. 1). The propeller was modelled as a cylindrical volume in the ADer as explained in 2.4.2.

ANSYS Meshing 17.2 was used for meshing 3D geometry and three grids were developed to assess the grid convergence. The Grid Convergence Index (GCI) and the y^+ number were used in the grid-independence solution evaluation (see Section 3.2).

2.4.2. Setup

All the CFD simulations assumed a single isothermal (38 °C) and incompressible fluid as the primary phase. The single-phase was defined as a non-Newtonian fluid using the Ostwald-de-Waele submodel with K = 0.0789 and $n - 1$ = -0.585.

The selected turbulence model was the Shear Stress Transport (SST) turbulence model developed by Menter, (1994) which is very robust and widely used. The SST model is a two-equation eddy-viscosity turbulence model that combines the k-ε turbulence model (in the free shear flow) and the k-ω turbulence model near walls. The advantage of the SST model *versus* k-ε lies in a better description of the shear stress in the wall through k-ω turbulence model wall treatment. The boundary conditions are described in Table 3.

A momentum source approach was set for the intermittent propeller operation. A cylindrical subdomain was used to replace the propeller geometry and contained a momentum source to drive fluid movement. The volumetric momentum source, M (kg m^{-2} s^{-2}), can be calculated according to the propeller technical sheet with the following expressions:

$$M = \frac{\rho}{V_S}\left(\frac{q}{D_a}\right)^2 \tag{24}$$

where D_a is the actual diameter of the blades (m), ρ is the fluid density (kg m^{-3}) and V_S (m^3) is the volume of the cylindrical subdomain. The propelled flow rate, q (m^3/s), can be obtained as:

$$q = D_a\sqrt{\frac{\omega}{\omega_o}\frac{F_o}{\rho}} \tag{25}$$

Table 3
Boundary conditions (see the flow rates in Table 1).

Patch	Boundary Type	Value
Inlet	Inlet: Mass Flow Rate	Inflow + Heat Exchanger Flow
Outlet	Outlet: Mass Flow Rate P = 1 atm	Inflow
Heat Exchanger Suction	Outlet: Mass Flow Rate	Heat Exchanger Flow
Dynomix 1	Inlet: Mass Flow Rate	45% of Dynomix Flow
Dynomix 2	Inlet: Mass Flow Rate	55% of Dynomix Flow
Dynomix Suction	Outlet: Mass Flow Rate	Dynomix Flow
Wall	Wall: Non-Slip Wall	–
Top	Wall: Free Slip Wall	–

being F_o the design thrust force (N), ω_o the rotational speed (rpm) for the propeller and ω is the actual rotational speed. The propeller was set by a thrust force of 1500 N, a cylinder diameter of 1.5 m, and a cylinder length of 0.2 m. The momentum source resulted in 4244 kg m^{-2} s^{-2}.

2.4.3. Solver and convergence

The ANSYS CFX solver is based on the finite volume method. All the scenarios had the same outline: firstly, a steady-state simulation was run to solve the hydrodynamics of a particular scenario. When the steady-state finished, a transient simulation was run to solve the transport of the tracer inside the ADer.

2.4.3.1. Steady-state simulations. Steady-state simulation was applied to accurately obtain the hydrodynamics of the studied mixing configurations by focusing on analysing sludge behaviour and detecting slow-velocity zones. High-resolution schemes were set as advection and turbulence schemes. To terminate the numerical calculations, different criteria were met in all the steady-state simulations:

1. At least 15,000 iterations with a time step of 1 s were set.
2. A reliable convergence criterion based on the root mean square (RMS) residual of 1×10^{-5} was adopted.
3. All the monitor points, the value of the different parameters at several points located around the geometry, were under 5% of the final value in the last 100 iterations
4. The solution imbalances in the conservation equations (conservation of mass, momentum, energy) were less than 0.001% for all the equations

2.4.3.2. Transient simulations: Inert tracer experience. After the steady-state simulation, the hydrodynamics calculation was frozen and a transient simulation was run to solve the tracer's transport equation. These simulations were performed to study the mixing and homogenisation in the different scenarios. The real tracer experience with lithium was reproduced: an additional variable was introduced into the domain and a short pulse with the total mass was introduced through the inlet nozzle. Its transport equation was defined as (ANSYS CFX, 2017):

$$\frac{\partial(\rho\varphi)}{\partial t} + \nabla(\rho U\varphi) = \nabla\left(\left(\rho D_\phi + \frac{\mu_t}{Sch_t}\right)\nabla\varphi\right) + S_\varphi \quad (26)$$

where U is the fluid velocity, ρ is the fluid density, ϕ is the concentration, φ is the conserved quantity per unit mass (ϕ /ρ), S_ϕ is the volumetric source term (zero in this case), D_ϕ is the kinematic diffusivity for the scalar (m^2/s), μ_t is the turbulent viscosity (kg/m s) and Sch_t is the turbulence Schmidt number (-). LiCl kinematic diffusivity was set at 2,919 $\times$ 10^{-9} m^2/s (Holz et al., 2000) and a Schmidt Number of 0.9 was chosen (Bujalski et al., 2002).

A variable time step was implemented with Eq. (27) and (28) (Climent et al., 2018):

$$t_i = t_0 r^i \quad (27)$$

$$T = \sum_{i=1}^{N} t_i = t_0 \frac{1 - r^N}{1 - r} \quad (28)$$

where i is the iteration number, t_i is the time step, t_0 is the initial time step, and r is the increasing rate so that Eq. in (27) gives the size of every time step. The total simulation time (T) was calculated with Eq. (28) where N is the total number of iterations. t_0, r and T were set as 0.1 s, 1.002, and 76 days respectively. Previous equations were used to reduce the simulation time and to apply a variable time step (shorter time step in the first iterations and a longer time step as simulation progressed).

3. Results and discussion

This section is about the analysis of digester performance based on the CFD simulations. Firstly, details of the different simulations and their corresponding operating conditions are presented. Then the validity of each simulation is evaluated according to conventional techniques, such as grid independence analyses and tracer studies. Once the validity of the proposed simulations was established, a detailed study of the so-called base scenario was performed. Its hydrodynamic behaviour was analysed by pointing out the main characteristics of these tank types (compartmented structure and fast circumferential velocity), as well as its efficiency to achieve homogeneous mixing. This base scenario served to analyse the influence of the two main operational parameters that can be changed in practice: recirculation rate and internal propeller activation. Finally, a comprehensive ADer performance assessment was made, including the design and mixing parameters described in Section 2.2.

Readers are referred to the Supplementary Material to find extended results.

3.1. Outline of the CFD simulations

To provide full insight into the global hydrodynamic behaviour and the influence of the operational parameters on ADer performance, several CFD simulation scenarios were conducted (see Fig. 2):

Scenario A100: it is the base scenario and was run with the DYNOMIX recirculation flow set in the plant (680 m^3/h) with the propeller switched off. As the ADer currently operates 162 h per week in this scenario, it is particularly interesting given its strong influence on residence time, settling, mixing, etc. It was used to conduct the grid convergence study (Section 3.2) and the tracer validation (Section 3.3), and to study the DYNOMIX system's basic hydrodynamics (Section 3.4).

Scenarios A200, A50, and A0: these scenarios were run using recirculation flows higher and lower than in the base scenario to study their influence on ADer performance. The variation in the recirculation flow in relation to the base scenario (RF) is specified in Fig. 2.

Scenario B100: The propeller is switched on 6 h per week to avoid dead volumes forming. To study its start-up influence, a transient simulation (comprising 1-hour evolution) was performed by taking the base scenario as the initial condition, A100.

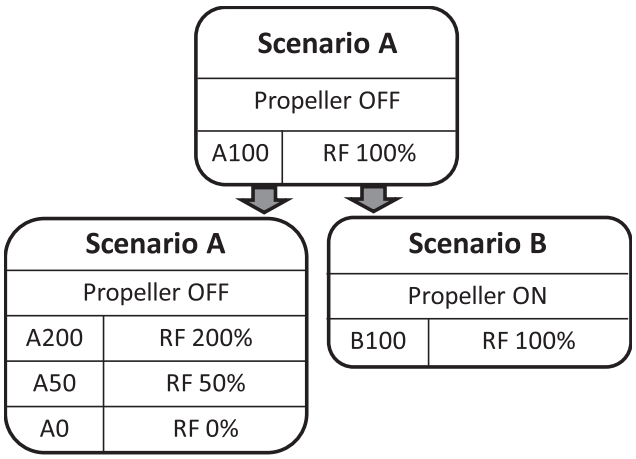

Fig. 2. Scheme of the CFD simulations.

3.2. Mesh quality

The different mesh properties that can influence mesh quality are summarised in Table S4. To ensure the mesh independency of the CFD results, a grid sensitivity study was carried out based on the GCI (Roache, 1998). The results provided by the intermediate grid were considered to be mesh independent as the GCI was below 3 %when calculated between the two finer meshes. A more detailed explanation of the GCI calculation can be found in the Supplementary Material.

3.3. Tracer test and global hydraulic validation of the model

The tracer test yielded a mean residence time of 19.6 days and short-circuiting of 12% of the total influent flow while no dead volumes were observed (Climent et al., 2019).

As in Terashima et al., (2009), the tracer test was used to validate the CFD simulation. For this purpose, a tracer pulse was set at the ADer's inlet in the A100 scenario. A transient simulation that spanned several days provided the calculated tracer curve. The plot in Fig. 3 compares the resulting E curve (A100) to the experimental one, which indicated a good agreement between them, especially for long times for which an RMS error of about 0.04 ppm was calculated. This agreement stands for the global validation of the base scenario, which can reproduce a full-scale ADer's hydrodynamics. In addition, a detailed analysis of the A100 curve at the beginning (see Fig. 3 for details) depicted minor internal recirculation or short-circuiting before the first tracer sample was taken. This hydraulic defect in the A100 scenario fitted the experimental short-circuiting detected in the tracer test.

3.4. Hydrodynamic behaviour of the base scenario

The base scenario's hydrodynamics is particularly important because the ADer normally works under these conditions. The CFD solutions allow the user to determine how dead volumes are formed and possible inhomogeneous mixing, but also provides more accurate knowledge about the inside flow behaviour and its implications during the process performance. This work proposes identifying three main ADer regions with very specific hydrodynamic characteristics for each zone to point out possible compartmental modelling. The mixing behaviour was studied by relating it to the local mixing parameters in Section 2.3.2 and evaluating the different global mixing parameters from Section 2.3.3 with the transient simulation results.

3.4.1. The ADer's compartmental structure

A careful examination of the velocity field in the tank volume suggested it can be divided into three regions: a cylindrical region along the vessel's axis (labelled as 1 in Fig. 4), and two annular regions at different heights, numbers 2 and 3.

The first region is referred to as the CORE because it is located in the centre of the vessel. The limits of this region were clearly noted from the circumferential velocity contours shown in Fig. 5a, and its

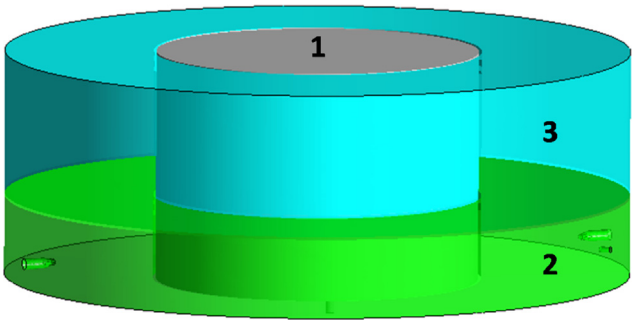

Fig. 4. Three regions defined in the vessel according to hydrodynamics: CORE of the vessel (1); DYNOMIX region (2) and TFR (3).

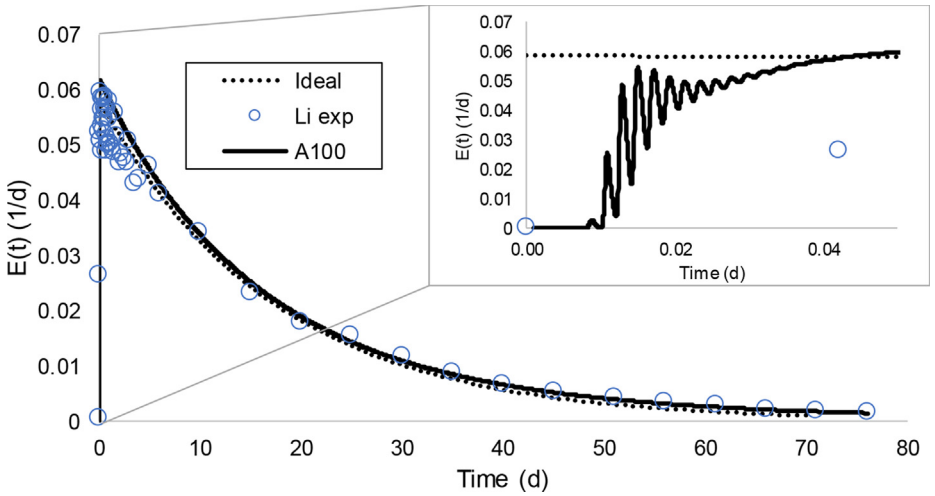

Fig. 3. Experimental, ideal and the A100 E curve in the outlet.

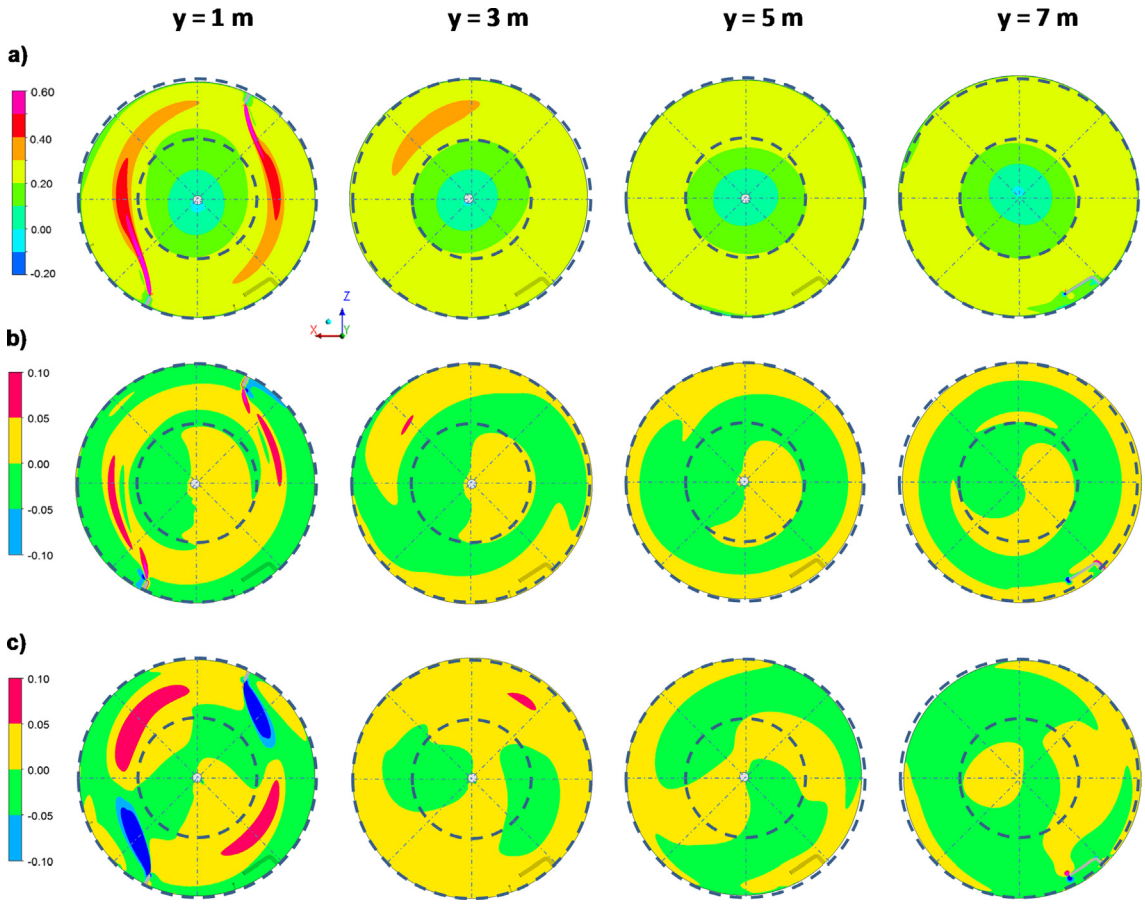

Fig. 5. Velocity contours (m/s) in different horizontal planes. The circumferential component is depicted in (a), the axial component in (b) and the radial velocity in (c). Note: a positive circumferential velocity means clock-wise movement, while a negative one denotes counter-clockwise movement. Positive axial velocity is upward velocity, while the negative one is downward velocity. Positive radial velocity indicates an outward movement, while a negative one denotes movement towards the centre.

frontier was about 6 m away from the ADer axis. The CORE zone was a region with slow circumferential velocity and upward and downward antisymmetrical flows dominated by fast and quite uniform circumferential velocity.

The second region is located close to the ground and surrounds the CORE. It is referred to as the DYNOMIX region because its hydrodynamics is strongly impacted by recirculation jets. The circumferential velocity contours (Fig. 5a) at several heights helped to establish the upper boundary of this region as being 3 m high, where the circumferential velocity to the ground increased due to recirculation jets. In the axial component (see Fig. 5b), a secondary flow moved sludge upwards near the CORE region and downwards near the wall. As the DYNOMIX flow entered the tank directed towards the centre of the vessel, the radial component of velocity was negative (Fig. 5c). But as the DYNOMIX flux circulated, it deviated towards the wall. So radial velocity was positive and quite quickly diluted the influent.

The third region is located above the second and is named the Turbulent Flow region (TFR) as its circumferential profile resembles that of a fully-developed turbulent flow (see Section 3.4.2 for more details). The circumferential velocity was almost uniform in this region and a local influence of the DYNOMIX suction pipe occurred at a height of 7 m (see Fig. 5a). The axial component (see Fig. 5b) was about one order of magnitude lower than the circumferential velocity. A secondary flow rotated in the opposite direction of the secondary flow in the DYNOMIX region. For axial velocity, the radial component was one order of magnitude lower than the circumferential component.

Readers are referred to the Supplementary Material for more information about secondary flows, streamlines and an extended description of compartments.

3.4.2. Circumferential flow: Turbulent vortex structure

From previous discussions, it was apparent that the circumferential velocity was typically one order of magnitude higher than the other velocity components across the whole digester, so flow basically spun around the ADer's axis. As in most rotating systems, the development of a vortex-like structure was expected. Fig. 6a and b show the circumferential velocity (v_θ) and angular circumferential velocity ($\omega = v_\theta/r$) for several profiles located at different heights on a vertical plane (Fig. 6c). The circumferential velocity distribution in the CORE region looked like a vortex, and the almost constant angular velocity supported such behaviour. Several mathematical models have been proposed to describe the distribution of tangential velocities in the core of a free vortex. Tangential velocities increase linearly from the rotation axis up to a maximum value at radius R_C, and decrease from this point outwardly and proportionally to the inverse of the radius. A simple laminar vortex model, like Burgers' vortex (Burgers, 1948), can represent this behaviour. In Fig. 6a, the dashed black line depicts the simplified version of Burger's model applied to this case. The velocity profiles in the CORE region (radial distance approximately below R_c = 8 m) closely matched the laminar vortex structure, for which velocity increased linearly with the radial distance (i.e. at a constant angular velocity, indicating rigid-like motion). In contrast, the profiles in the DYNOMIX and TF regions strongly deviated from the laminar

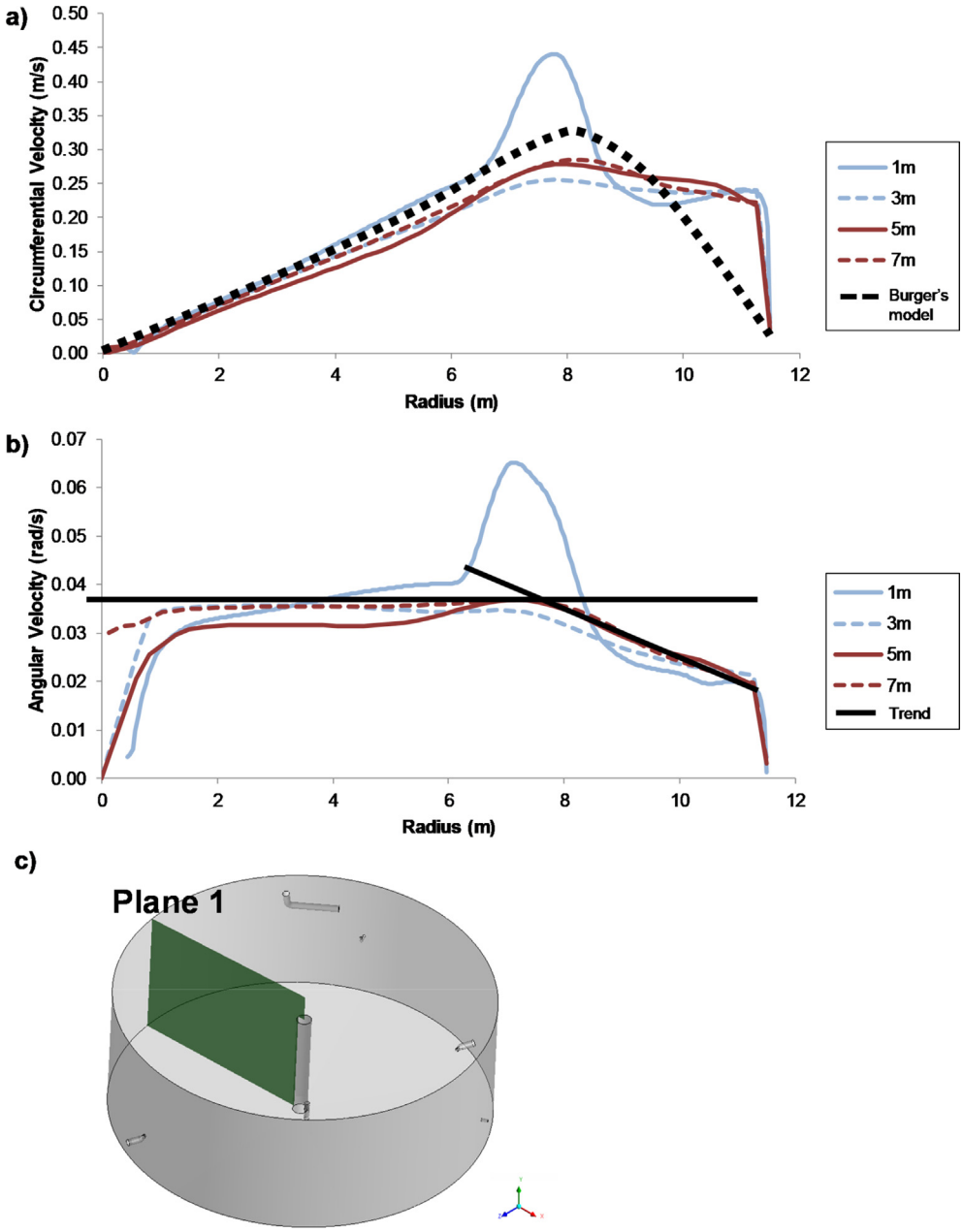

Fig. 6. (a) Circumferential velocity profile, (b) angular velocity profile at different heights and trending lines and (c) location of the plane containing the profiles in the plots.

vortex profile. The profile at 1 m clearly indicated that the DYNOMIX jet broke the laminar vortex structure in the DYNOMIX region. The profiles at 3 m, 5 m and 7 m showed that the circumferential velocity remained almost constant after reaching its maximum value at a radial distance of about 8 m, while the angular velocity linearly decreased. Near the wall, the circumferential velocity indicated the same behaviour as the velocity distribution on the boundary layer of a fully-developed turbulent channel. Hence the velocity profile fitted a power-law expression as in (White, 2011):

$$w(r) = w_o\left(1 - \frac{r}{R_{\text{ADer}}}\right)^{n_\tau} \tag{29}$$

where r stands for the radial coordinate, $w(r)$ is the circumferential velocity component, R_{ADer} is the ADer radius, w_o denotes the circumferential velocity immediately beyond the boundary layer velocity, and n_τ is the turbulent exponent constant, with a value close to 1/7. For our ADer, that constant was 1/7.6 (see Figure S4 for the fitting procedure). In summary, the outer regions, DYNOMIX and Turbulent Flows were seen as a fully-developed turbulent channel, while the inner region (the CORE region) resembled a vortex structure. All the regions had secondary flows that helped to understand the mixing process, but their velocities were one order of magnitude lower.

3.4.3. Design parameters assessment

In this section, the design parameters were analysed (Section 2.3.1) by means of the power consumption of the ADer under study (see Table 4) compared to the recommended design parameters (see the values in brackets in Table 4):

The DYNOMIX system inputs 7.3 kW, i.e. 22 kW with 33% efficiency, and the impeller uses 3.5 kW, but only 6 h per week. So this ADer has longer DVTT (5.10 h) and a lower UP (2.13 W/m^3) compared to the design values. This means that bad mixing performance could be expected due to a slow recirculation flow with

Table 4
Design parameters for the ADer.vs US EPA, (1979) in brackets.

HRT (d)	DVTT (h)	UP (W/m^3)	$\bar{G}$ (s^{-1})
17.0 (15–30)	5.10 (30–40 min)	2.13(5–8.3)	5.15 without propeller// 6.2 with propeller (50–80)

low pumping power. Nonetheless, the experimental tracer experiment depicted CSTR performance with slight short-circuiting. Therefore, it stands that proper mixing with less power input can be achieved with good local power input distribution. These disagreements between real performance and design parameters can be partially explained by impeller intermittent performance, which avoids dead volumes forming. Additionally, these disagreements suggest that DVTT and UP are design parameters that are not the most significant when defining the mixing efficiency of an ADer. For example, the same recirculation flow applied to two different ADers with the same volume will have the same DVTT and UP, but different mixing degrees depending on the recirculation flow distribution with nozzles.

The aim of the global RMS velocity gradient was to relate the ideal mixing power to good mixing performance in a global parameter. On the one hand by using Eq.(6), the global parameters, i.e. average dynamic viscosity of 0.0789 Pa s and real power input, $\bar{G}$ stood for 5.15 s^{-1} without the propeller and 6.27 s^{-1} with the propeller. These values were one order lower than the proposed design values and, thus, the ADer's mixing performance would be poor according to $\bar{G}$. On the other hand according to the design standards, the range of power that should be applied in the ADer to achieve between 50 s^{-1} and 80 s^{-1} would be between 683 kW and 1976 kW, extremely high compared to that installed in the real system.

This clearly agrees with other authors (Sindall et al., 2013; Wu, 2014), who have pointed out that the global RMS velocity gradient cannot accurately characterise the local mixing of full-scale ADers. Hence, this parameter should not be used for designing ADers' mixing systems.

In summary, the design parameters can be useful for comparing different ADers, but fail to define the mixing degree because it depends on the mixing systems' efficiency and location. Additionally, DVTT is only applicable with hydraulic mixing ADers, and UP and $\bar{G}$ are too global to capture the local mixing phenomena that take place in ADers.

3.4.4. Local mixing analysis

Large ADers usually display heterogeneous hydraulic behaviour, and although the global analysis is useful, tools are needed to analyse local behaviour and its effects on mixing. The local mixing produced by a recirculation system can be studied by means of two local parameters: the local RMS velocity gradient and the α_{DME}. The local RMS velocity gradient, Eq. (9), was computed by turbulent kinetic energy dissipation per unit mass and local viscosity, from the CFD results. Fig. 7a shows a histogram that depicts the distribution of the local RMS velocity gradients for every ADer region. As expected, the CORE region exhibited the poorest mixing because the RMS velocity gradients remained below 0.2 s^{-1}. The TFR had higher velocity gradients and the gradient velocity of most of its volume was between 0.2 and 0.8 s^{-1}. The TFR's mixing was more

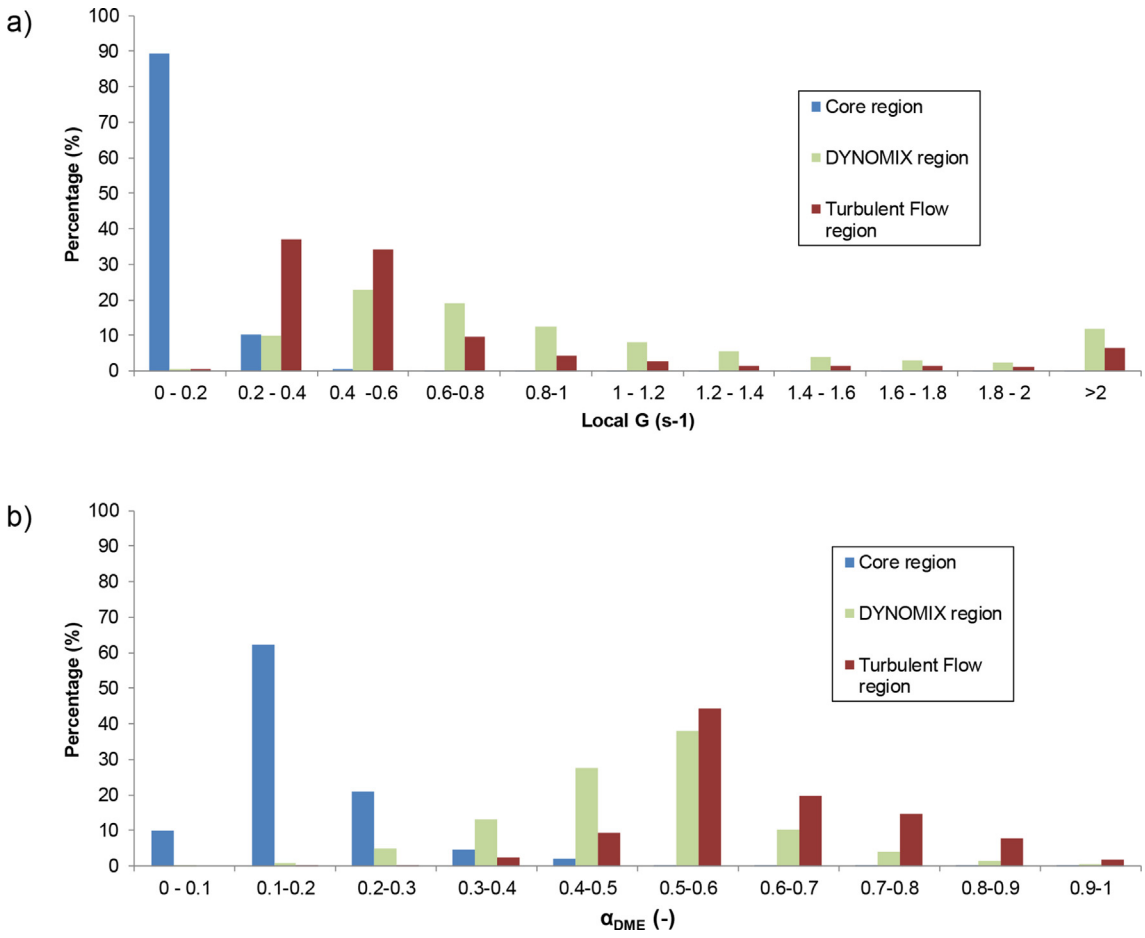

Fig. 7. Histograms for (a) the RMS velocity gradient and (b) the Dispersive Mixing Efficiency for every region.

homogeneous than in other regions. Conversely, the gradients in the DYNOMIX region were widely distributed, with more than 2 s^{-1} on 10% of its volume thanks to the action of jets, with a peak value of 20 s^{-1} near the DYNOMIX nozzles. These values in the digester were several orders of magnitude below the design threshold of 50–85 s^{-1}(which is recommended in the design parameters). This shows that lower local RMS velocity gradients can also generate proper mixing in full-scale ADers as the tracer depicted CSTR performance.

Fig. 7b shows the α_{DME}'s distribution for every region. In the CORE region, this value was lower than 0.5, so, mixing came from sludge's solid–liquid laminar vortex. α_{DME} increased in the outer regions with values above 0.5, with the mixing in these regions arising from the shear flow in the DYNOMIX region (towards values < 0.5) and the dispersive flow in the TFR (towards values > 0.6).

Overall, the results of both local parameters agreed with the turbulent structure described in Section 3.4.2. While the CORE region has a rotational flow without local mixing due to a laminar vortex, the outer regions had better local mixing and included a turbulent channel flow produced by the recirculation flow and its interaction with the outer wall. Moreover, the TFR was the ADer's most efficient mixing region as its local RMS Velocity gradients were significant and widely dispersed.

3.4.5. Global mixing parameters assessment

Having studied local mixing, the homogeneity of the components inside the ADer can be studied by the tracer curve. Hence the tracer experience enables the study of the UI, the mean tracer concentration and the second-order moment of the tracer distribution in the different ADer regions.

On a semilogarithmic scale, Fig. 8 depicts the tracer concentration average (Fig. 8a), the UI curves for each region and the whole ADer (Fig. 8b), and the normalised second-order moments along the three directions (Fig. 8c).

In a first step, the average concentration and the global UI of the whole ADer was calculated so that it provided a global t_{UI}. However, the calculation of these parameters in the different regions provided a greater degree of detail on tracer's movement: the tracer entered sequentially in the DYNOMIX region, then in the TFR and lastly in the CORE region.

Nevertheless, the analysis of the central moments of the tracer concentration provides further information on the tracer path and its dispersion over time without a regions' analysis: the circumferential moment rapidly increased over the axial and radial second-order moments, which implies that it was the preferential direction. The radial direction was the disadvantageous one for being the last on achieving a constant value.

From these curves, homogenisation times were obtained for each parameter: On the one hand, t_{UI} could be obtained for each region and, as the CORE region was the last to accomplish complete mixing, the ADer's t_{UI} was 54 min. On the other hand, from the normalised second-order moments, this homogenisation time was reached lastly at 54.6 min in the radial direction. Note that both homogenisation times were almost equal.

3.5. Anaerobic digester performance assessment

In this section, the scenarios described in Section 3.1, were evaluated following the same structure as the previous one.

3.5.1. Compartmental structure

As described in Section 3.4.2, the circumferential velocity was the most important velocity component in the base scenario's compartmental structure. So, this velocity component was used in sketching the compartmental structure of the different CFD scenarios (see Figures S9-S12).

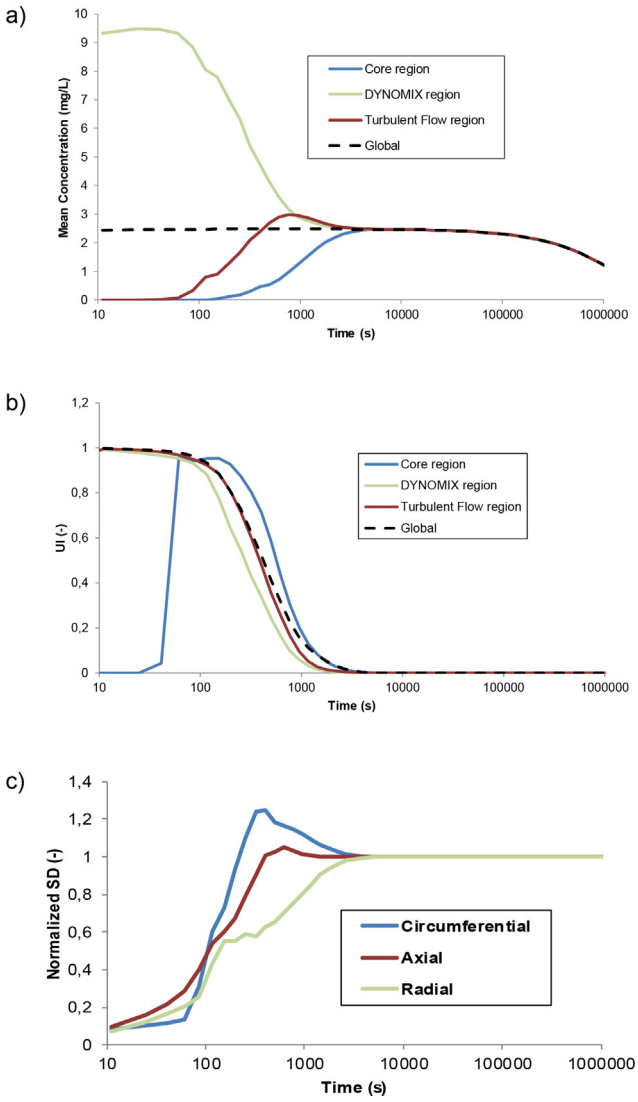

Fig. 8. Time evolution of the (a) Mean tracer concentration, (b) Uniformity index in CORE, DYNOMIX and TF regions and the global ADer and (c) Normalized second order central moment curves along the three spatial directions.

Briefly, the compartmental structure of the A100 scenario remained in the A50 and A200 cases, and was similar in the B100 scenario. In scenario B100, the impeller effect brought about considerable internal recirculation inside the CORE region, and the radial and axial velocities increased in the zone directly affected by the impeller. Without the recirculating flow, A0 showed a very slow circumferential velocity and, thus, the compartmental structure was not maintained.

3.5.2. Circumferential flow: Turbulent vortex structure

As in the base scenario, the circumferential velocity was one order of magnitude over the other velocity components in scenarios A50, A100, A200 and B100. On the one hand, it is noticeable that, although B100 had slower circumferential velocities than A200 from a 6 m radius to the wall, it was almost equal for both scenarios in the CORE region (see the circumferential velocity at 5 m height in Fig. 9a). On the other hand, low circumferential velocities were always located in the CORE region, so this would most likely create areas of settlement and dead volume in reality. Nevertheless in the A0 scenario, all the velocity components had the same magnitude (Fig. 9a).

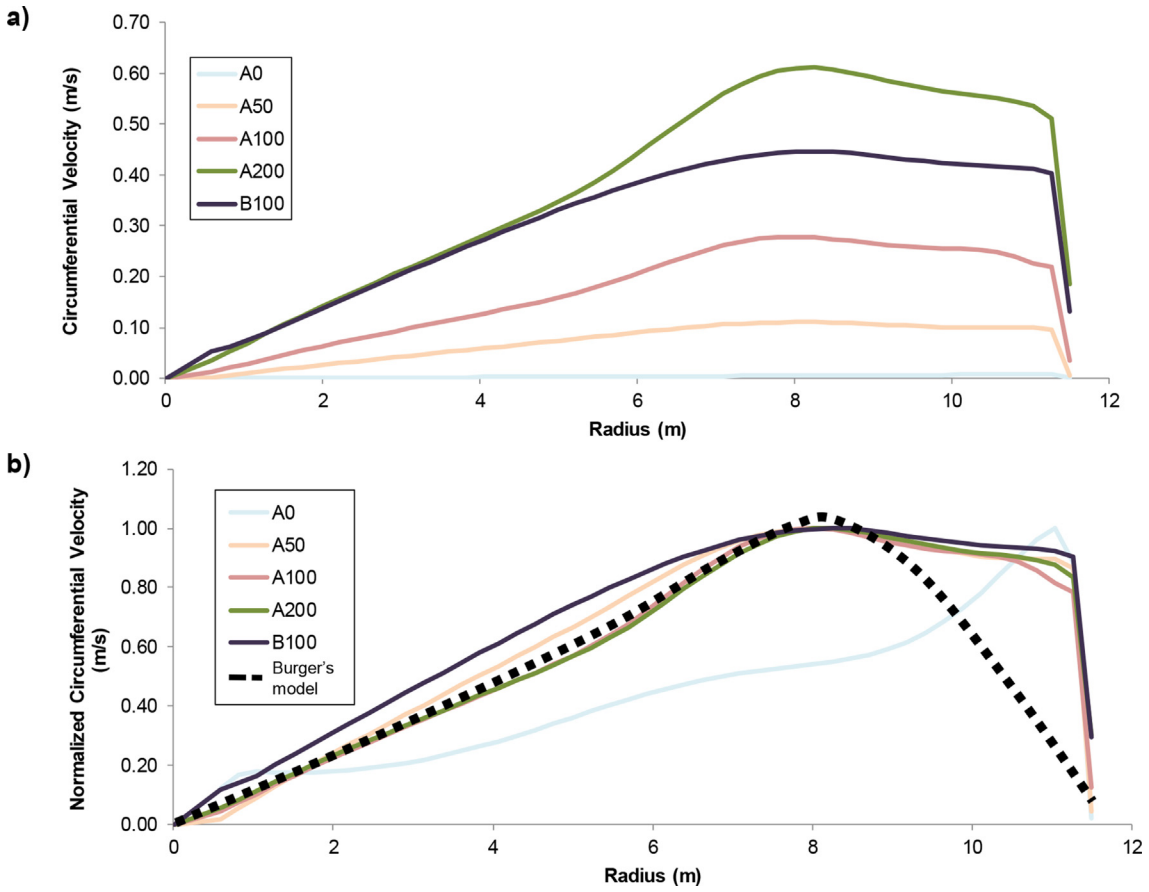

Fig. 9. (a) Circumferential velocity and (b) normalized circumferential velocity at the 5 m height for the different scenarios.

Fig. 9b depicts the normalised circumferential velocity in the different scenarios and a typical laminar vortex profile (dashed line). As seen in Section 3.4.2, the CORE region in scenarios A50, A100, A200, and B100 agreed with the laminar vortex. Nonetheless, the A0 scenario did not follow any vortex profile in the inner region, but showed a turbulent profile in the region near the wall as all the scenarios did.

3.5.3. Local mixing analysis

The local RMS Velocity gradient and α_{DME} are assessed in the different scenarios for the various regions (see Fig. 10). According to the local RMS velocity gradient, in A0 it remained at low gradients in every region. In the scenarios with DYNOMIX system, the local RMS velocity gradient was encouraged and B100 was the scenario with better mixing in the CORE region as a result of the source of the propeller's momentum. For the α_{DME}, the volume distribution showed that mixing moved towards a rotational shear flow in the DYNOMIX region and towards a dispersive flow in the TFR. In the CORE region, mixing came from the rotational flow, i.e. $< 0\alpha_{DME}.5$, in all scenarios except for A0 where there was a shear flow. Nonetheless, the type of mixing in A0 can be neglected due to the local gradients lower than 0.2 s^{-1}.

Therefore, the joining of the local RMS velocity gradient and α_{DME} implied excellent parameters for describing mixing performance in ADers. Additionally, B100 was established as the best for the mixing of the CORE region.

3.5.4. Global mixing parameters assessment

The global mixing parameters are studied using the tracer test simulations performed on the different scenarios. A complete 76-day RTD was obtained (see Fig. 11) and avoided having to carry out tracer experiments for every scenario which can reduce the study's cost. Fig. 11 shows that the RTD was similar and without peaks in A100, A200, and B100. Thus their global hydraulic performance came close to a CSTR. Conversely, A0 and A50 clearly showed a tracer's fluctuation and a sharp peak, respectively, so major hydraulic defects appeared in them (Fig. 11 detail): the fluctuation in A0 could be an internal recirculation or short-circuit, while the sharp peak at A50 could be a short-circuit. These short-circuits should be taken into account when adding co-substrates because the influent flow would leave the ADer almost immediately without dilution or treatment. Thus if co-substrates are to be introduced, scenarios A100, A200 and B100 will dilute them.

Then, the global mixing parameters were computed: Figures S13 and S14 depict the mean tracer concentration and UI for all the scenarios and Figure S15 depicts the normalised second-order moments at each direction. Table 5 shows the time when the tracer entered each region (from the second to the fourth column) and the homogenisation times according to the UI and the second-order moments.

The tracer's behaviour in the DYNOMIX scenarios (A50, A100, A200 and B100) was very similar to the base scenario description done in Section 3.4.5: the inlet flow introduced the tracer directly into the DYNOMIX region and the recirculation flow drove it to the DYNOMIX region. Then the tracer enters the TFR and lastly the CORE. This pattern could be stated with time when the tracer enters each region in Table 5.

The homogenisation times with the UI, t_{UI}, and second order moments are shown in Table 5. Similar times were obtained with both parameters and an alike pattern was described: the lower the DYNOMIX recirculation flow rate, the longer the homogenisation time; thus A0 had the highest one. Note that B100 and A200

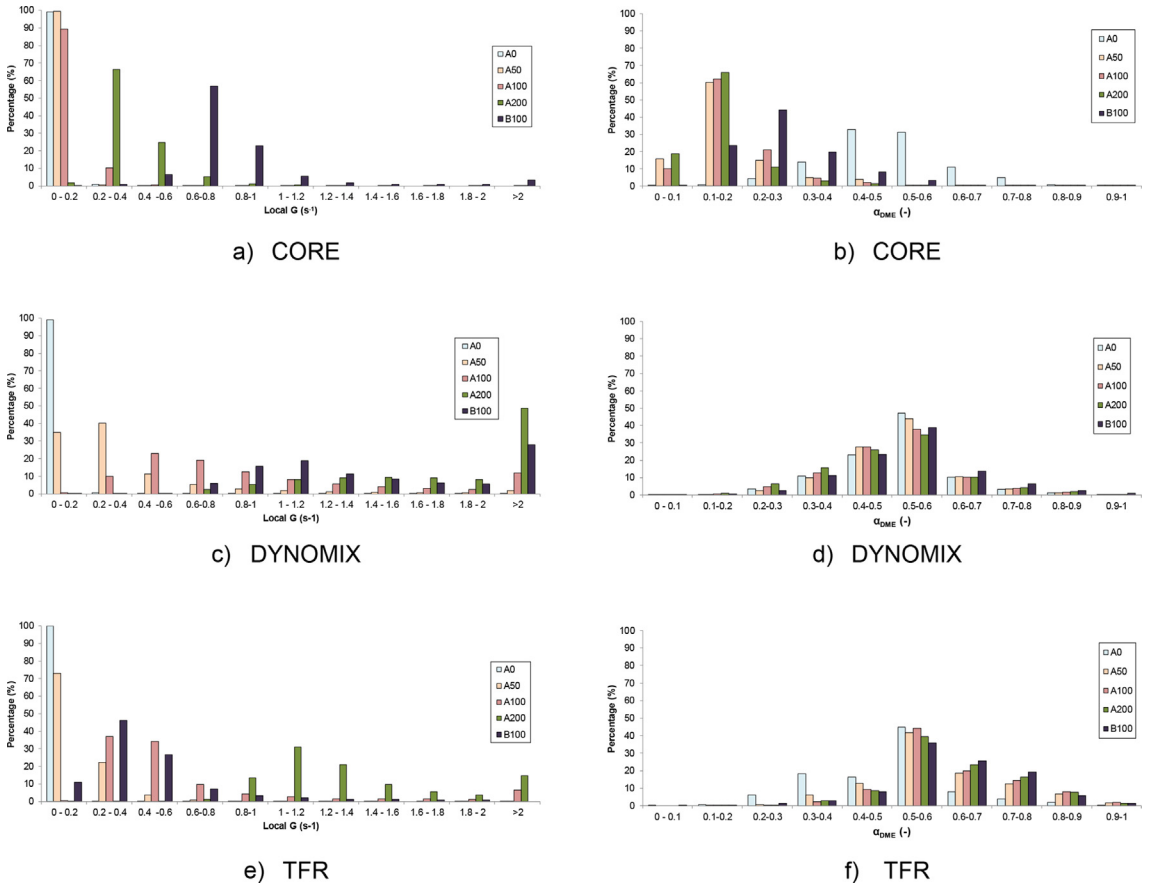

Fig. 10. Histograms for the local RMS velocity gradient (a,c,e) and α_{DME} (b,d,f) for every scenario at different regions.

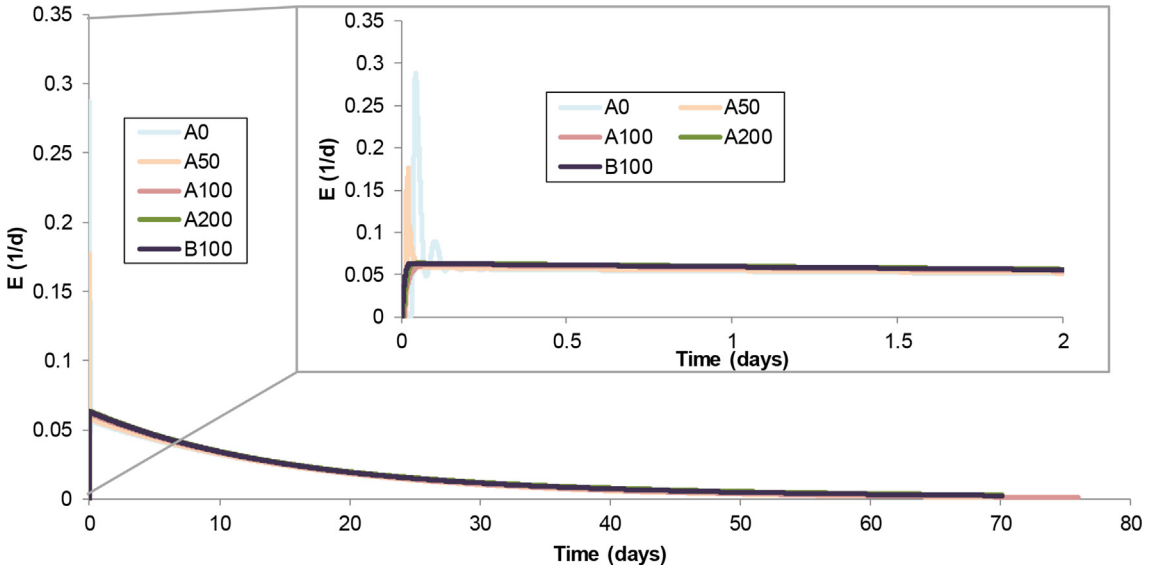

Fig. 11. E curve of lithium in the outlet in scenarios A0, A50, A100, A200 and B100, complete and detailed until day 2.

reduced the homogenisation time by about 50% compared to A100 but, B100 was the scenario with the shortest homogenisation time.

Based on these global parameters, it is easy to draw some conclusions about ADer mixing. The RTD and global parameters showed that mixing in A200 and B100 was similar, but the energy use in A200 was much higher (44 kW) than in B100 (25.5 kW). Therefore, if mixing is to be maximised, it should be done with B100.

Overall, the UI and second-order moments led to similar conclusions and homogenisation times, although the UI findings were established thanks to the compartmental UI study. However, second-order moments provide local information with a global

Table 5
First time that the tracer entered each region (T_0) and the homogenisation time with the UI and the second-order moment for the whole CFD simulation.

Scenario	T_0CORE Region	T_0 DYNOMIX Region	T_0TF Region	UI Homogenisation Time (min)	Second-order Moment Homogenisation Time (min)
A0	24	0	400	366.7	223.3
A50	200	0	90	91.7	91.7
A100	150	0	60	54	54.7
A200	100	0	25	25	30
B100	85	0	40	21.7	24.2

parameter without having to resort to compartmentalisation. Additionally, second-order moments state the direction with less mixing and, thus, shows the direction in which mixing in bad mixing scenarios should be encouraged. In short, the agreement between both parameters endorses the robustness and consistency of second-order moments.

4. Conclusions

The hydrodynamics of an ADer with an external recirculation pump mixing system was studied with CFD models and tracer test results. Non-Newtonian single-phase CFD simulations were performed to assess the recirculation system (DYNOMIX) and a 3-blade propeller in several scenarios: without recirculation flow, A0; with 50%, 100% and 200% recirculation flow, A50, A100, and A200, respectively; with 100% of recirculation flow and a 3-blade propeller, B100. The base scenario (A100) was thoroughly verified in a transient state to accurately reproduce the actual operating conditions, which makes its global validation unique with a complete experimental RTD of 76 days.

The hydrodynamics of the different scenarios and several mixing parameters were analysed and the following conclusions were drawn:

- CFD models' hydrodynamics showed a very fast circumferential velocity driven by liquid recirculation jets. Three compartments were proposed: Firstly, the CORE region at the centre of the ADer is drawn by slow velocities and a laminar vortex structure. Then in its surroundings, a fully-developed turbulent channel is shown: the DYNOMIX region, where DYNOMIX jets offer the fastest ADer velocities, and the TFR, with slower velocities than the DYNOMIX region, but faster ones than those of the CORE.
- The design parameters, i.e. DVTT, HRT, UP, and G, were evaluated. According to the experimental RTD and current energy demands, the authors agree with literature works that have designed parameter thresholds and should be reviewed: they fail to define energy needs and are too global to show local mixing.
- Concerning local mixing parameters, the local RMS velocity gradient and α_{DME} define the mixing degree and mixing type, respectively. They were studied in each region of the different scenarios. Employing both parameters to define ADers' mixing performance is encouraged. The CORE region comes over as the lowest mixed region and the DYNOMIX region as the highest mixing one in all the scenarios. B100 is the most efficient scenario for CORE's mixing due to the propeller's momentum
- Second-order moments are proposed as a new global mixing parameter to study ADers' mixing degree in each direction. Its results were compared to the UI in the different scenarios and regions. Second-order moments are able to provide geometrical local mixing information without compartmentalisation so they are simpler and more valuable than the UI. With the second-order moments, the radial direction is negligible during the mixing process, which can be enhanced in mixing strategies, i.e. in B100.
- Homogenisation times were established with the UI and second-order moments. The actual ADer (A100) was homogenised in less than 1 h. The effect of increasing recirculation (A200) and switching on the propeller (B100) was evaluated. Both scenarios depict similar homogenisation times. Hence both scenarios are likely to barely influence the overall process, and can be used to rapidly dilute inhibiting compounds or cosubstrates. Nonetheless, B100 is more appreciated given the very high energy use in A200.
- Finally, if energy consumption needs to be reduced, A50 could be considered with an influent nozzle modification to avoid its short-circuit. In addition, the likeliness of dead volume formation would need to be reviewed.
- The analysis of the scenarios shows that the additional mixing provided by propellers is more effective than an increase in the recirculation flow in ADers with this liquid recirculation system type. Propellers reduce slow-velocity areas and, consequently, minimise the appearance of dead volumes inside ADers. Thus further studies should focus on investigating the most efficient angle of recirculation nozzles to avoid dead volumes

The foregoing conclusions state that CFD simulations help to understand full-scale ADers' hydrodynamics and transient simulations with virtual tracer tests help to carry out exhaustive analyses of mixing patterns.

CRediT authorship contribution statement

Rosario Arnau: Writing – original draft, Investigation. **Javier Climent:** Writing – original draft. **Raúl Martínez-Cuenca:** Writing – original draft, Investigation. **Jorge Rodríguez:** Writing – review & editing. **Sergio Chiva:** Conceptualization, Writing – review & editing, Supervision.

Declaration of Competing Interest

The authors declare that they have no known competing financial interests or personal relationships that could have appeared to influence the work reported in this paper.

Acknowledgements

The authors thank the work carried out in the Spanish anaerobic digesters and published in (Climent et al., 2019).

Funding: This work was supported by the Conselleria de Educación, Investigación, Cultura y Deporte from Generalitat Valenciana (ACIF/2016/255). Jorge Rodríguez work at Khalifa University (United Arab Emirates) was supported by the Sustainable Bioenergy Research Consortium (SBRC) under Award No. EX2019-003

Appendix A. Supplementary material

Supplementary data to this article can be found online at https://doi.org/10.1016/j.ces.2021.117392.

References

ANSYS CFX, 2017. User Manual, Release 17.2.

Appels, L., Baeyens, J., Degrève, J., Dewil, R., 2008. Principles and potential of the anaerobic digestion of waste-activated sludge. Prog. Energy Combust. Sci. 34 (6), 755–781. https://doi.org/10.1016/j.pecs.2008.06.002.

Bridgeman, J., 2012. Computational fluid dynamics modelling of sewage sludge mixing in an anaerobic digester. Adv. Eng. Softw. 44 (1), 54–62. https://doi.org/10.1016/j.advengsoft.2011.05.037.

Bujalski, J.M., Jaworski, Z., Bujalski, W., Nienow, A.W., 2002. The Influence of the Addition Position of a Tracer on CFD Simulated Mixing Times in a Vessel Agitated by a Rushton Turbine. Chem. Eng. Res. Des. 80 (8), 824–831. https://doi.org/10.1205/026387602321143354.

Burgers, J., 1948. A mathematical model illustrating the theory of turbulence. Adv. Appl. Mech. 1, 171–199 https://doi.org/10.1016/S0065-2156(08)70100-5.

Changgen Luo, 1997. Distribution of Velocities and Velocity Gradients in Mixing and Flocculation Vessels: Comparison Between LDV Data and CFD Predictions.

Cholette, A., Cloutier, L., 1959. Mixing efficiency determinations for continuous flow systems. Can J Chem Eng 1959:35. Can. J. Chem. Eng. 37 (3), 105–112.

Climent, J., Basiero, L., Martínez-Cuenca, R., Berlanga, J.G., Julián-López, B., Chiva, S., 2018. Biological reactor retrofitting using CFD-ASM modelling. Chem. Eng. J. 348, 1–14. https://doi.org/10.1016/J.CEJ.2018.04.058.

Climent, J., Kiser, A., Arnau, R., Pita, C., Bonmatí-blasi, A., Chiva, S., 2019. Comparison between Potassium Bromide and Lithium Chloride as feasible tracer for assessing hydraulic performance in anaerobic digesters. in: 8th International Conference on Tracers and Tracing Methods.

Craig, K.J., Nieuwoudt, M.N., Niemand, L.J., 2013. CFD simulation of anaerobic digester with variable sewage sludge rheology. Water Res. 47 (13), 4485–4497. https://doi.org/10.1016/j.watres.2013.05.011.

Dapelo, D., Bridgeman, J., 2018. Assessment of mixing quality in full-scale, biogas-mixed anaerobic digestion using CFD. Bioresour. Technol. 265, 480–489. https://doi.org/10.1016/j.biortech.2018.06.036.

Dustin, J.S., Hansen, C.L., 2012. Completely Stirred Tank Reactor Behavior in an Unmixed Anaerobic Digester: The Induced Bed Reactor. Water Environ. Res. https://doi.org/10.2307/42569473.

Holz, M., Heil, S.R., Sacco, A., 2000. Temperature-dependent self-diffusion coefficients of water and six selected molecular liquids for the calibration in acccurate HNMR PFG m. Phys. Chem. Chem. Phys. 2, 4740–4742. https://doi.org/10.1039/b005319h.

Hurtado, F.J., Kaiser, A.S., Zamora, B., 2015. Fluid dynamic analysis of a continuous stirred tank reactor for technical optimization of wastewater digestion. Water Res. 71, 282–293. https://doi.org/10.1016/j.watres.2014.11.053.

Khapre, A., Munshi, B., 2016. Data on the mixing of non-Newtonian fluids by a Rushton turbine in a cylindrical tank. Data Br. 8, 1416–1420. https://doi.org/10.1016/j.dib.2016.08.023.

Kleerebezem, R., 2014. In: Biomass as a Sustainable Energy Source for the Future: Fundamentals of Conversion Processes. John Wiley & Sons, Inc, Hoboken, NJ, pp. 441–468. https://doi.org/10.1002/9781118916643.ch14.

Levenspiel, O., 1999. Chemical Reaction Engineering. Ind. Eng. Chem. Res. 38 (11), 4140–4143.

Li, S., Xin, F., Li, L., 2017. Reaction Engineering. Jonathan Simpson.

Manas-Zloczower, I., 1994. Studies of mixing efficiency in batch and continuous mixers. Rubber Chem. Technol. 67, 504–528. https://doi.org/10.5254/1.3538687.

Mendoza, A.M., Martínez, T.M., Montañana, V.F., López-Jiménez, P.A., 2011. Modeling flow inside an anaerobic digester by CFD techniques. Int. J. Energy Environ. 2, 963–974.

Menter, F.R., 1994. Two-Equation Eddy-Viscosity Turbulence Models for Engineering Applications. AIAA J. 32 (8), 1598–1605.

Meroney, R.N., Colorado, P.E., 2009. CFD simulation of mechanical draft tube mixing in anaerobic digester tanks. Water Res. 43 (4), 1040–1050. https://doi.org/10.1016/j.watres.2008.11.035.

Monteith, H.D., Stephenson, J., 1981. Mixing efficiencies in full-scale anaerobic digesters by tracer methods. J. Water Pollut. Control Fed. 53, 78–84.

Papoulis, A., 1984. Probability, random variables and stochastic processes with errata sheet: solution, Technometrics. McGraw-Hill, New York. https://doi.org/10.2307/1266379

Paul, E.L., Atiemo-Obeng, V.A., Kresta, S.M., 2004. Handbook of industrial mixing. New Jersey.

Roache, P.J., 1998. Verification of codes and calculations. AIAA J. 36, 696–702.

Schramm, G., 1994. A Practical Approach to Rheology and Rheometry, 2nd Editio. ed. https://doi.org/10.1017/CBO9781107415324.004

Sindall, R., Bridgeman, J., Carliell-Marquet, C., 2013. Velocity gradient as a tool to characterise the link between mixing and biogas production in anaerobic waste digesters. Water Sci. Technol. 67, 2800–2806. https://doi.org/10.2166/wst.2013.206.

Smith, L.C., Elliot, D.J., James, A., 1993. Characterisation of mixing patterns in an anaerobic digester by means of tracer curve analysis. Ecol. Modell. 69 (3-4), 267–285. https://doi.org/10.1016/0304-3800(93)90030-V.

Tchobanoglous, G., Burton, F., Stensel, H., 2003. Wastewater engineering treatment and reuse.

Tchobanoglous, G., Stensel, H.D., Burton, F.L., 2004. Wastewater Engineering: Treatment and Reuse, 4th Editio. ed. McGraw-Hill. https://doi.org/10.1007/s13398-014-0173-7.2

Terashima, M., Goel, R., Komatsu, K., Yasui, H., Takahashi, H., Li, Y., Noike, T., 2009. CFD simulation of mixing in anaerobic digesters. Bioresour. Technol. 100 (7), 2228–2233. https://doi.org/10.1016/j.biortech.2008.07.069.

US EPA, 1979. Process Design Manual for Sludge Treatment and Disposal, 625/1-79–0. ed. EPA, Cincinnati, Ohio.

White, F.M., 2011. Fluid mechanics. McGraw Hill.

Wu, B., 2014. CFD simulation of gas mixing in anaerobic digesters. Comput. Electron. Agric. 109, 278–286. https://doi.org/10.1016/j.compag.2014.10.007.

Wu, B., 2011. CFD investigation of turbulence models for mechanical agitation of non-Newtonian fluids in anaerobic digesters. Water Res. 45 (5), 2082–2094. https://doi.org/10.1016/j.watres.2010.12.020.

Wu, B., 2010a. CFD simulation of gas and non-Newtonian fluid two-phase flow in anaerobic digesters. Water Res. 44 (13), 3861–3874. https://doi.org/10.1016/j.watres.2010.04.043.

Wu, B., 2010b. CFD simulation of mixing in egg-shaped anaerobic digesters. Water Res. 44 (5), 1507–1519. https://doi.org/10.1016/j.watres.2009.10.040.